Nonlinear Emission of Microcavity Polaritons in the Low Density Regime

P. Senellart* and J. Bloch

Laboratoire de Microstructures et de Microélectronique, C.N.R.S, B.P. 107, 92225 Bagneux Cedex, France

(Received 3 August 1998)

We present polariton emission measurements as a function of the excitation power in a III-V semiconductor microcavity. In a large range of power the polariton emission exhibits a clear nonlinear behavior. Since its energy, in-plane dispersion, and radiation pattern remain unchanged, no polariton bleaching occurs. A model, including phonon assisted relaxation stimulated by the polariton final state population, accurately describes the experimental variations of the nonlinearity amplitude and threshold with the detuning. [S0031-9007(98)08222-2]

PACS numbers: 71.36.+c, 42.55.Sa, 71.35.Lk

If the quasibosonic nature of excitons has given rise to many theoretical works [1], no clear experimental manifestation of that bosonic character has ever been evidenced. In semiconductor microcavities containing quantum wells (QW), where excitons and photons can be strongly coupled, new opportunities for observing a bosonic behavior appear. In this strong coupling regime (SCR), first observed in 1992 [2], excitons and photons form mixed states, named cavity polaritons [3]. The Fermi golden rule does not hold anymore for the light emission inside the cavity, and the front emission detected from outside the sample is due to the leakage through the top mirror of the polariton photon part. Therefore, in the SCR, photon stimulated emission can no longer occur.

In Ref. [4] a new lasing mechanism, called exciton boser, is proposed: The relaxation of large in-plane wave-vector excitons toward the lower polariton state, via acoustic phonon emission, is stimulated by the polariton final state population. This implies that the exciton and carrier density is small enough for phase space filling and screening to be negligible, so that polaritons can be considered as quasibosons. Moreover, since polaritons can have a small effective mass, the boser effect is expected to be observed before bleaching.

Recently, a laserlike emission has been observed in semiconductor microcavities containing QWs [5–7]. However, it did not occur in the SCR because of a large excitation power. Polaritons were bleached, and the system had transited to the weak coupling regime. The polariton line was shifted toward the uncoupled cavity mode, and the calculated exciton Bose commutator was well below 1. We present here measurements of a polariton nonlinear emission in the low density SCR which give strong indications for the existence of a boser. This experiment is performed on a III-V semiconductor microcavity under continuous nonresonant excitation, using very small excitation powers. Over a large range of excitation power, the polariton line does not spectrally shift and presents a nonlinear variation of the integrated intensity. We develop a simple rate equation model, including phonon assisted relaxation stimulated by the quasibosonic polariton final state population. We obtain a good description of our results, especially when varying the detuning between the cavity mode and the exciton.

The sample has been grown by molecular beam epitaxy. It consists of a λ GaAs cavity containing a single 8-nm $Ga_{0.95}In_{0.05}As$ QW, surrounded by two Bragg mirrors. The top (bottom) mirror contains 20 (24) $Ga_{0.9}Al_{0.1}As/AlAs$ $\lambda/4$ pairs. The spatial variation of the layer thicknesses allows one to tune the cavity with respect to the QW exciton by changing the spot under examination on the sample. Reflectivity performed at 1.4 K evidences an anticrossing between the cavity mode and the heavy-hole exciton line with a Rabi splitting of 3.5 meV. At resonance, the upper (lower) branch linewidth amounts to 0.51 meV (0.23 meV) showing the high sample quality.

Photoluminescence (PL) measurements are performed at 1.4 K for various excitation powers. The sample is excited with a cw Ti:sapphire focused into a spot of 30–40 μm. The emission is dispersed with a monochromator and detected with a multichannel Si detector. To avoid broadening induced by the sample spatial inhomogeneity and the excitation inhomogeneity inside the laser spot, we use a spatial selection corresponding to a 20 μm size on the sample. Moreover, we use an angular selection: We detect light emitted in a 4° full external angle. This reduces broadening induced by the polariton in-plane dispersion [8].

The excitation is nonresonant: The laser field is fixed at 1.75 eV, far beyond the upper limit of the Bragg mirror stop band, where the reflectivity lies at about 0.3. Figure 1 presents PL spectra measured for a detuning δ between the exciton and the cavity mode of -4 meV [$\delta = E_c - E_x$, where E_c (E_x) is the energy of the uncoupled cavity mode (exciton)]. The spectra are divided by the excitation power and measured for four different excitation powers. For the three smallest powers, the upper polariton intensity varies linearly with the excitation power, whereas a nonlinearity is observed on the lower polariton.

Figure 2(a) shows the integrated intensity over power of the upper and lower branch for $\delta = -4$ meV while Fig. 2(b) shows the lower branch energy and linewidth.

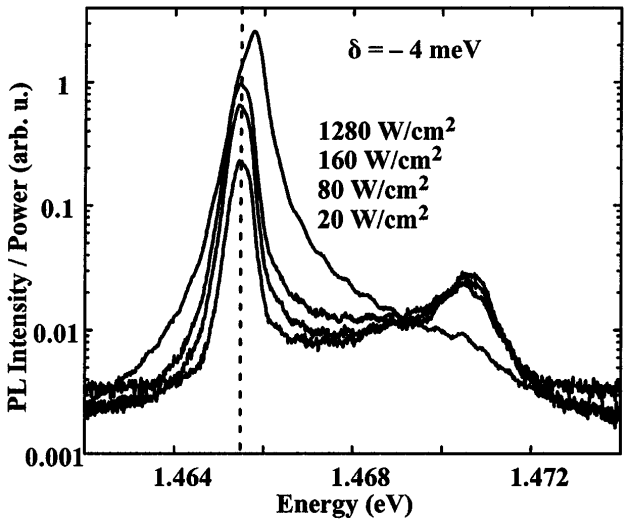

FIG. 1. PL spectra normalized to the excitation power measured for $\delta = -4$ meV for four different excitation powers.

For incident powers greater than 200 W/cm^2, the lower branch is blueshifted and broadened. The carrier density corresponding to 200 W/cm^2 lies at about 4×10^{10} cm^{-2}, i.e., close to the threshold for phase space filling and exciton screening [9,10]. The lower branch blueshift is the signature of the transition from the strong to the weak coupling regime. For much larger power, a sharp nonlinearity occurs, associated with a narrowing of the line. This should correspond to the standard threshold for photon stimulated emission in the weak coupling regime as previously observed [5–7].

For incident powers lower than 200 W/cm^2, a strong nonlinearity is observed on the integrated emission intensity of the lower branch while its energy remains constant within 0.1 meV. Furthermore, this first threshold lies at about 10 W/cm^2, corresponding to a carrier density of only 2×10^9 cm^{-2}, far below bleaching threshold.

Finally, we performed angle resolved PL measurements. Figure 3 presents the integrated intensity and energy of the lower branch as a function of the in-plane wave vector for three different excitation powers. The lowest one corresponds to the nonlinear threshold, the intermediate to the nonlinear regime, whereas the largest power is well above screening threshold. As long as the lower polariton energy remains constant, the in-plane dispersion and the radiation pattern are unchanged, whereas for high excitation powers inducing a blueshift of the lower polariton line, both in-plane dispersion and radiation pattern are modified. All of these features allow us to conclude that the nonlinear behavior observed for small excitation powers occurs in the SCR.

Let us now consider the evolution of this nonlinearity with δ. It could be observed for various negative detunings $\delta \leq -2$ meV. However, closer to resonance or for positive detunings, the emission of both branches was linear as long as no screening occurred. Figure 4 presents the lower branch integrated intensity over excitation power as a function of the excitation power for various negative detunings. The inset allows a precise determination of the transition between strong and weak coupling for each detuning. The nonlinearity threshold increases when going toward large negative δ, i.e., to a more photonlike lower polariton. At the same time, the amplitude of the nonlinearity increases.

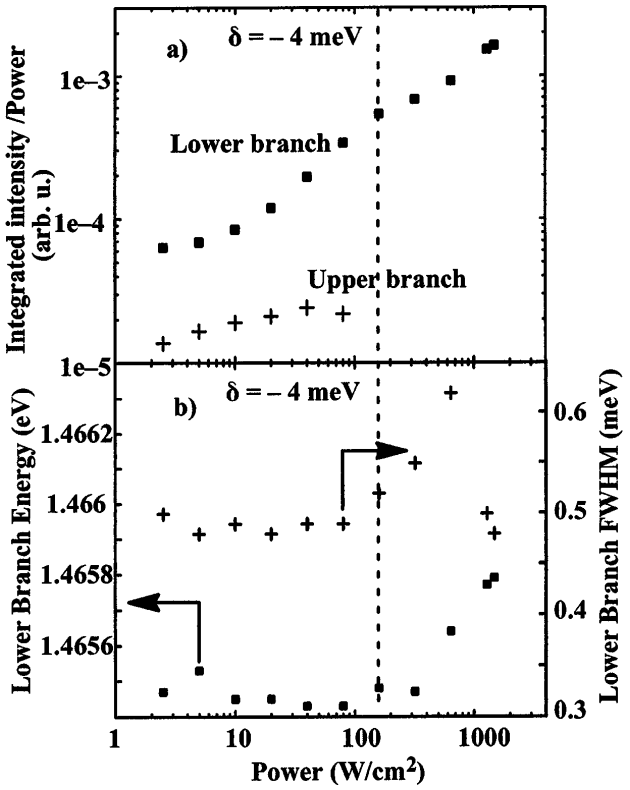

FIG. 2. (a) + (■): Upper (lower) branch integrated PL intensity over power as a function of the excitation power: (b) +: Lower branch full width at half maximum (FWHM), and ■: lower branch energy as a function of the excitation power. All of these measurements are done for $\delta = -4$ meV. The vertical dashed line represents the polariton bleaching threshold.

As the first nonlinearity occurs for very low density, the exciton Bose commutator is very close to 1 [7]. To test the hypothesis of a boser mechanism, we compare the data in Fig. 4 with a rate equation model which includes the polariton bosonic character. In this model, the phonon assisted relaxation of large in-plane wave-vector excitons is stimulated by the polariton final state population [5]. We consider three manifolds: One represents the reservoir of exciton states with large in-plane wave vectors and population N_R (close to the uncoupled exciton energy). The excitation directly populates these states with a pump rate P_R. The two other manifolds represent the upper and lower polariton with populations N_U and N_L.

The polariton interaction with acoustic phonons is proportional to its exciton part c_{exc}, whereas the photon escape probability is proportional to its photon part c_{phot} [11]. These components vary with δ. The population time evolution is described as follows:

$$\frac{dN_R}{dt} = P_R - \frac{N_R}{\tau_R} + c_{\text{exc}}^L\{AN_L n_T(E_{\text{exc}} - E_L) - BN_R(N_L + 1)[n_T(E_{\text{exc}} - E_L) + 1]\}$$
$$+ c_{\text{exc}}^U\{AN_U[n_T(E_U - E_{\text{exc}}) + 1] - BN_R(N_U + 1)n_T(E_U - E_{\text{exc}})\}$$
$$+ D[2c_{\text{exc}}^L c_{\text{exc}}^U N_U N_L + (c_{\text{exc}}^L N_L + c_{\text{exc}}^U N_U)N_R + 2(c_{\text{exc}}^L N_L)^2 + 2(c_{\text{exc}}^U N_U)^2]$$
$$\frac{dN_L}{dt} = -\frac{c_{\text{phot}}^L N_L}{\tau_{\text{phot}}} - c_{\text{exc}}^L\{AN_L n_T(E_{\text{exc}} - E_L) - BN_R(N_L + 1)[n_T(E_{\text{exc}} - E_L) + 1]\}$$
$$- D[c_{\text{exc}}^L c_{\text{exc}}^U N_U N_L + c_{\text{exc}}^L N_L N_R + 2(c_{\text{exc}}^L N_L)^2].$$

A similar equation is considered for N_U.

E_{exc}, E_L, and E_U are the energy of the uncoupled exciton, lower polariton, and upper polariton, respectively. $A \cdot c_{\text{exc}}$ is the scattering rate via acoustic phonons from the upper or lower polariton toward the reservoir and $B \cdot c_{\text{exc}}$ from the reservoir toward the polariton states. A and B take into account both the average strength of the interaction with acoustic phonons and the density of states of the final state. We take $A^{-1} = 15$ ps and $B^{-1} = 400$ ps in accordance with Refs. [11,12]. D introduces collisions between two polaritons or between a polariton and a reservoir exciton. $\tau_{\text{phot}} = 6.6$ ps is the photon escape time out of the cavity (deduced from the cavity linewidth) and $\tau_R = 200$ ps is the mean radiative lifetime of reservoir excitons [13]. $n_T(E)$ is the thermalized phonon population of energy E at temperature T. We assume that phonon thermalization is very efficient. The terms $(N_L + 1)$ and $(N_U + 1)$ reflect the polariton quasibosonic character. The reservoir bosonic character has been neglected as this manifold gathers a large number of states individually weakly populated. If N_L and N_U were neglected with respect to 1, the emission would be linear with P_R, which does not correspond to our experimental results.

We calculate the stationary solution of these nonlinear equations and deduce the emission intensity as a function of P_R. For small excitation powers, N_L and N_U are small enough for the nonlinear terms in the rate equations to be neglected: The calculated behavior is linear. When N_L becomes close to 1 while N_U remains small, the relaxation from the reservoir toward the lower branch becomes very efficient and results in an exponential increase of N_L. Without collisions, the lower branch would finally collect all additional carriers injected in the clamped reservoir, reaching a second linear regime. However, the calculated slope of the nonlinearity and its total amplitude are larger than in the experimental data. The introduction of collisions results in a balance between

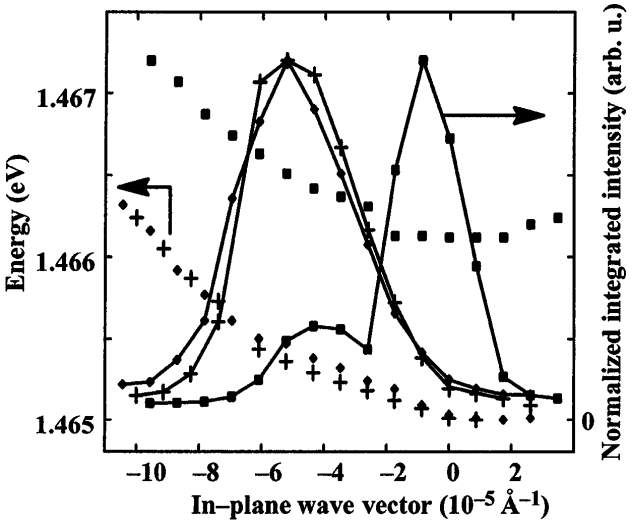

FIG. 3. Left axis: Energy of the lower branch as a function of the in-plane wave vector for an excitation power of (+) 10 W/cm^2, (◆) 100 W/cm^2, and (■) 1250 W/cm^2. Right axis: Normalized integrated intensity of the lower branch as a function of the in-plane wave vector for an excitation power of (—+—) 10 W/cm^2, (—◆—) 100 W/cm^2, and (—■—) 1250 W/cm^2.

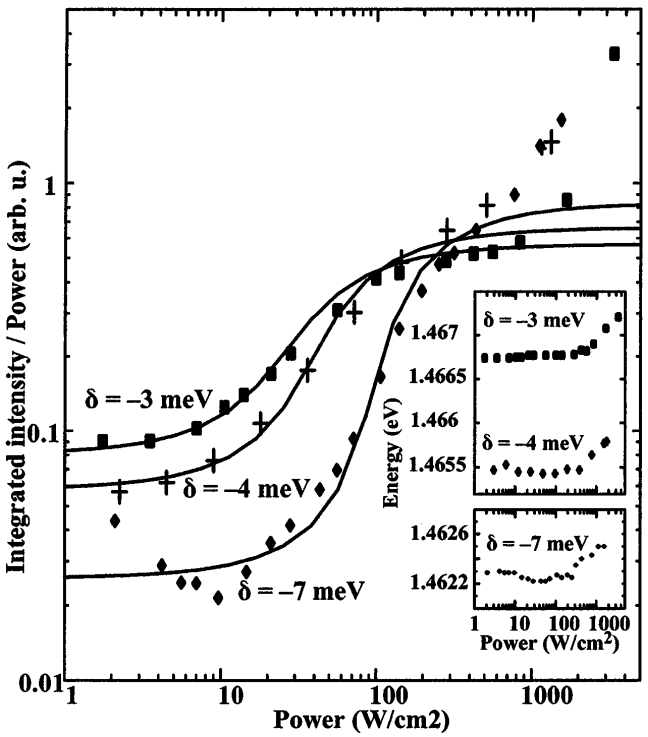

FIG. 4. Experimental integrated intensity over power as a function of the excitation power for a detuning of (◆) −7 meV, (+) −4 meV, and (■) −3 meV. Full lines: Calculated intensities over power for the same three detunings. Inset: Energy of the lower branch as a function of the excitation power for the same three detunings.

stimulated polariton relaxation and collisions so that both N_L and N_R grow linearly.

In Fig. 4, the experimental data are superimposed to the calculated values. The only fitting parameter, used for the three calculated curves, is $D^{-1} = 407$ ps. Recent picosecond measurements give the same order of magnitude for this collision coefficient [14]. An excellent agreement is obtained for the whole strong coupling region. As expected, the experimental data deviate from calculation for larger powers corresponding to polariton bleaching. When going toward a photonlike polariton, interaction with phonons becomes less efficient. Thus, the first threshold and the amplitude of the nonlinearity increase because the polariton state is less occupied for small excitation powers.

According to our model, the nonlinearity results form the buildup of a lower polariton population with an occupation factor close to 1. Indeed, the estimated carrier density at threshold is about $4 \times 10^9\ \mathrm{cm}^{-2}$ for $\delta = -7$ meV. The corresponding ratio N_L/N_R amounts to 10^{-3}. This yields a threshold polariton density in the lower branch of $4 \times 10^6\ \mathrm{cm}^{-2}$. Assuming a thermal equilibrium of the lower branch population and taking into account its in-plane dispersion, the occupation factor of the zone center states is close to 1. Despite the simplicity of our model, the build up of the polariton population occurs for realistic densities. In the fermionic electron-hole correlation approach developed in [7], the exciton Bose commutator is close to 1 for densities considered here. It would be very interesting to see if this approach, including phonon interaction, can explain the nonlinear emission we observe, due to the buildup of a polariton population.

When $\delta > -2$ meV, no nonlinearity is observed. The lower branch density of states increases drastically so that the carrier density necessary to reach an occupation factor close to 1 exceeds the bleaching threshold. Moreover, the nonlinearity is never observed on the upper branch. Quick transfers from the upper branch to the large number of reservoir states at close energies [15] prevent the buildup of the polariton population. We did not try to describe this asymmetry between the upper and lower branch in our model. Finally, let us rule out the possibility of a photon amplification by localized states which would occur for negative detunings. This conventional stimulated emission would actually arise at the energy of the uncoupled photon mode, which is obviously not the case.

In summary. the nonlinear emission presented here occurs in the SCR as proved by the unchanged polariton energy, radiation pattern, and dispersion in this excitation power range. The evolution of the PL integrated intensity with the excitation power and detuning is well reproduced by a boser model, including relaxation stimulated by the polariton final state population. This model uses realistic carrier densities which correspond to an occupation factor close to 1. These are good indications of boser polariton behavior. New types of experiments are currently being performed to directly probe the polariton population. They should experimentally allow one to unambiguously identify the stimulation process.

We would like to thank our collaborators, B. Jusserand, J. Y. Marzin, R. Planel, V. Thierry-Mieg, and T. Freixanet for fruitful discussions and encouragement, and C. Weisbuch and H. Benisty for stimulating discussions.

Note added.—After the submission of this paper, Dang and co-workers [16] evidenced a laserlike behavior for small excitation powers in II–VI microcavities. It would be interesting to perform angle resolved measurements on their structure and compare their results to our simple boser model.

*Email address: pascale.senellart@12M.CNRS.FR

[1] For a review, see *Bose-Einstein Condensation*, edited by A. Griffin, D. W. Snoke, and S. Stringari (Cambridge University Press, New York, 1995).
[2] C. Weisbuch *et al.*, Phys. Rev. Lett. **69**, 3314 (1992).
[3] See various early articles in *Confined Electrons and Photons New Physics and Applications*, edited by E. Burstein and C. Weisbuch, NATO ASI Ser. B Vol. 340 (Plenum, New York, 1995).
[4] A. Imamoglu and R. J. Ram, Phys. Lett. A **214**, 193 (1996).
[5] S. Pau *et al.*, Phys. Rev. A **54**, R1789 (1996).
[6] H. Cao *et al.*, Phys. Rev. A **55**, 4632 (1997).
[7] M. Kira *et al.*, Phys. Rev. Lett. **79**, 5170 (1997).
[8] R. Houdré *et al.*, Phys. Rev. Lett. **73**, 2043 (1994).
[9] S. Schmitt-Rink, D. S. Chemla, and D. A. B. Miller, Phys. Rev. B **32**, 6601 (1985).
[10] R. Houdré *et al.*, Phys. Rev. B **52**, 7810 (1995).
[11] J. Bloch and J. Y. Marzin, Phys. Rev. B **56**, 2103 (1997).
[12] B. Sermage *et al.*, Phys. Rev. B **53**, 16 516 (1996).
[13] F. Tassone *et al.*, Phys. Rev. B **53**, R7642 (1996).
[14] T. Freixanet and B. Sermage (unpublished).
[15] J. J. Baumberg *et al.*, Phys. Rev. Lett. **81**, 661 (1998).
[16] Le Si Dang *et al.*, Phys. Rev. Lett. **81**, 3920 (1998).